JPPIPA 8(5) (2022)

Jurnal Penelitian Pendidikan IPA

Journal of Research in Science Education

http://jppipa.unram.ac.id/index.php/jppipa/index

Dual-Polarized PCF-SPR Sensor for Alcohol Detection at Low Temperature

Azhar[1], Khaikal Ramadhan[2], Dedi Irawan[1*]

[1]Department. of Physics PMIPA, FKIP, Universitas Riau Pekanbaru, Indonesia
[2]Department. of Physics, FMIPA, Institut Teknologi Bandung, Bandung, Indonesia

Received: September 19, 2022
Revised: Nivember 14, 2022
Accepted: November 27, 2022
Published: November 30, 2022

Corresponding Author:
Dedi Irawan
dedi.irawan@lecturer.unri.ac.id

DOI: 10.29303/jppipa.v8i5.2143

Abstract: We have observed a numerical simulation of the PCF-SPR sensor detecting alcohol concentration at low temperatures. The investigation was carried out using the finite element method on the PCF-SPR geometric structure. We use a simple geometry structure of the sensor by using fused silica and gold as the sensor's core and plasmonic material. Observations were made in the alcohol concentration range of 15%, 40%, 60%, and 70%. In the literature, we find the refractive index of each alcohol concentration and input its value into the proposed sensor. The proposed sensor shows that the sensor has a sensitivity in detecting alcohol concentrations at low temperatures of 91 nm/%. In the end, we obtained the optimal sensor components and the sensor can detect the alcohol concentration at low temperatures.

Keywords: PCF-SPR sensor; COMSOL multiphysics; Alcohol concentration; Low-temperature

Introduction

Optical components have tremendous advantages over electronic components, when it was first discovered that optical fiber was only used as a data transmission medium (Irawan et al., 2022). Optical fiber continues to experience significant developments to be applied in many fields. The need for this component continues to increase along with the times. Optical fiber can not only be applied in the field of communication but can also be applied as a component of optical sensors (Ramadhan & Saktioto, 2021; Ramadhan, 2020). Several optical sensor components that have reached the commercialization stage are single-mode fiber (SMF) and Bragg lattice fiber (FBG) (Mohapatra et al., 2022; Irawan et al., 2022; Irawan et al., 2022; Saktioto et al., 2021b). This optical sensor component can measure physical changes such as temperature, strain, pressure, displacement, force, and refractive index (Saktioto et al., 2021a). By utilizing a wide wavelength range, this component has a very high sensitivity, wide detection range, small size, and is resistant to electromagnetic wave interference (EM) (Korganbayev et al., 2018; Hsu et al., 2021).

Recently, with the development of optical fiber fabrication methods, a modern component with a unique structure was found, called photonic crystal fiber (PCF) (Irawan et al., 2022b). This component has an air cavity around the core and cladding. With the presence of this air cavity, a phenomenon that can be used in the world of communication and optical sensing (Irawan et al., 2022a). In the world of communication to produce PCF supercontinuum components, it has a high birefringence and has a material loss that can be adjusted according to its needs. Meanwhile, in the world of optical sensing, PCF is coated with plasmonic material to cause electron oscillation events on the sensor surface and also generate evanescent waves (Islam et al., 2021). Some of the plasmonic materials used in coating PCF are gold, silver, iron, and copper. Some researchers prefer to use gold in coating PCF because it is chemically stable. Meanwhile, the dielectric materials used in PCF are fused silica, Zeonex, and TOPAS (Mou et al., 2020, Sen et al., 2021, Irawan et al., 2022b).

How to Cite:
Azhar, A., Ramadhan, K., & Irawan, D. (2022). Dual-Polarized PCF-SPR Sensor for Alcohol Detection at Low Temperature. *Jurnal Penelitian Pendidikan IPA*, *8*(5), 2260–2265. https://doi.org/10.29303/jppipa.v8i5.2143

Several researchers have reported the geometric structure of the PCF-SPR sensor for various fields such as detecting refractive index, temperature sensing, magnetic field sensing, early sensing of cancer-infected cells, and sensing alcohol concentrations. Sensing the alcohol concentration is important to know the concentration level of the alcohol liquid. Several researchers have reported their work, among the sensors that have been reported sensing is based on the percentage of sensitivity (Rahman et al., 2021). In this work, we perform numerical simulations of the PCF-SPR sensor component in detecting the concentration of a mixture of alcohol and water at low temperatures. We observed that the resonance sensor wavelength shifts with changes in alcohol concentration.

Method

The finite element method (FEM) is used in this study, the first thing to do is to arrange the geometric structure of the PCF, arrange the air holes around the core and the PCF cladding after that arrange the analyte location, the thickness of the plasmonic material layer and the thickness of the PML as shown in Figure 1 geometric structure proposed sensor with 1(a) finite element sensor and 1(b) materials structure. The diameter of the sensor core is 5.875 µm. The size of the air hole contained in the core is distinguished in size, where the air hole closest to the gold layer has the largest size, namely d3, while the hole size at the next level is d2, while the air hole closest to the core has a diameter of d1 with their respective values are d1 = 0.4 µm, d2 = 0.5 µm, d3 = 0.7 µm.

The small size of the hole in the middle is intended to facilitate the excitation of surface plasmon polariton (SPP). In addition, this hole size will also cause lateral leakage. So that in the sensor design, the polarization can be adjusted in the middle and as desired. The distance between air holes d1 and d2 is 3.57 µm, while the distance between air holes d2 and d3 is 5.1 µm. This distance is based on the center of the hole to the center of the hole. This sensor design is also coated with gold plasmonic material with a thickness of 45 nm, then in this paper will also be carried out variations of the effect of gold thickness to optimize sensor performance. The thickness of the analyte section is set to 0.5 µm, the gold layer is right after the core layer, followed by the analyte layer and the last layer of this sensor is PML to concentrate electromagnetic waves at the center of the sensor and there is no wave leakage, PML has a thickness of 1 µm.

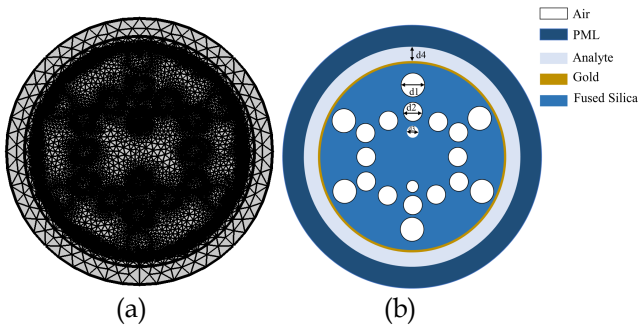

Figure 1. Geometric structure of PCF-SPR sensor, (a) finite element, (b) materials structure

Result and Discussion

Fused silica is the most commonly used PCF material, and is reported to have the best performance when compared to other materials such as TOPAS, Zeonex, etc. The sellmeier equation can be used in defining the fused silica material in the S-PCF-SPR design. The distribution of the refractive index for silica materials can be seen in equation 1.

$$n(\lambda)=\sqrt{1+\frac{0.696\lambda^2}{\lambda^2-0.0047}+\frac{0.408\lambda^2}{\lambda^2-0.014}+\frac{0.897\lambda^2}{\lambda^2-97.934}} \quad (1)$$

Where n is the refractive index of silica for each particular wavelength, is the wavelength that illuminates the surface of the S-PCF-SPR. The plasmonic material used to elicit the SPR effect on the PCF, the plasmonic material used in this study is gold, gold is chemically more stable than the environment but shows a wide resonance peak and this will harm the components. The Drude-Lorentz model is used to calculate the dielectric constant of gold which can be shown in equation 2 (Irawan, Ramadhan, Saktioto, Fitmawati, et al., 2022a).

$$\varepsilon_{au}=\varepsilon_{\infty}-\frac{\omega_D^2}{\omega(\omega+j\gamma_D)}-\frac{\Delta\varepsilon\Omega_L^2}{(\omega^2-\Omega_L^2)+j\Gamma_L\omega} \quad (2)$$

With Au being the gold permittivity value, and high frequency permittivity with a value of 5.9673, then is the plasma frequency, where D is the dumping frequency and D is the plasmon frequency which numerically has a value of 31.84π THz and 4227.2π THz and the oscillator power with symbol L = 1300.14π THz, and the spectral width is L = 209.72π THz. PCF that has air holes around the surface will cause loss when light passes through the surface. This confinement loss can be defined as equation 3 (Rifat et al., 2016).

$$L_c(dB/cm)=\left(\frac{4\pi f}{c}\right)\mathrm{Im}(n_{eff})\times 10^4 \quad (3)$$

Where Lc is the material confinement loss, with a value of 3.14, f = frequency, neff is the effective refractive index, and c is the speed of light. Meanwhile, PCF-SPR performance factors such as wavelength sensitivity can be defined in equation 4.

$$S_\lambda \left(nm / RIU \right) = \Delta\lambda_{peak} / \Delta n \quad (4)$$

Wavelength sensitivity shows how big the shift in the wavelength of the peak loss is for each change in the analyte's refractive index. A large shift for a small change in the refractive index of the analyte will show components that are ultra-sensitive and have high performance in differentiating changes in the refractive index of the analyte. Wavelength sensitivity also shows the difference in peak loss at a certain wavelength divided by the difference in the sensing refractive index (Lu et al., 2014). Another technique that is also used in characterizing sensor components is to find the amplitude sensitivity which can be defined in equation 5. In some literature we found the relationship between the concentration of a mixture of alcohol and water on the refractive index of the analyte, in Table 1 the data is presented for a temperature of 20 ^{0}C (Wu et al., 2017).

$$S_\lambda \left(1 / RIU \right) = \frac{1}{\alpha\left(\lambda, n_a\right)} \frac{\partial\alpha\left(\lambda, n_a\right)}{\partial n_a} \quad (5)$$

Based on Figure 1, it shows the distribution of the electric field on the surface of the PCF-SPR sensor, in 2(a) it is the left spp-mode and 2(b) is the right spp-mode. Spp-mode arises due to the presence of plasmonic material outside the PCF fiber layer. This material gives rise to electron oscillation events. Meanwhile, we find dual-polarization on the sensor, namely in Figure 2(c) for x-polarization and Figure 2(d) for y-polarization. Dual-polarization is obtained from 2D simulations using FEM, not all PCF-SPR components are dual-polarized, some researchers report that some PCF-SPR sensor components do not have dual-polarization, this occurs from inconsistent polarization on the sensor surface when detecting analytes (Shakya et al., 2022).

Table 1: Refractive Index of Ethyl Alcohol-water Mixtures at 20 ^{0}C

Ethyl Alcohol Amount (%)	Refractive Index
15	1.34361
40	1.35855
60	1.36336
70	1.36472

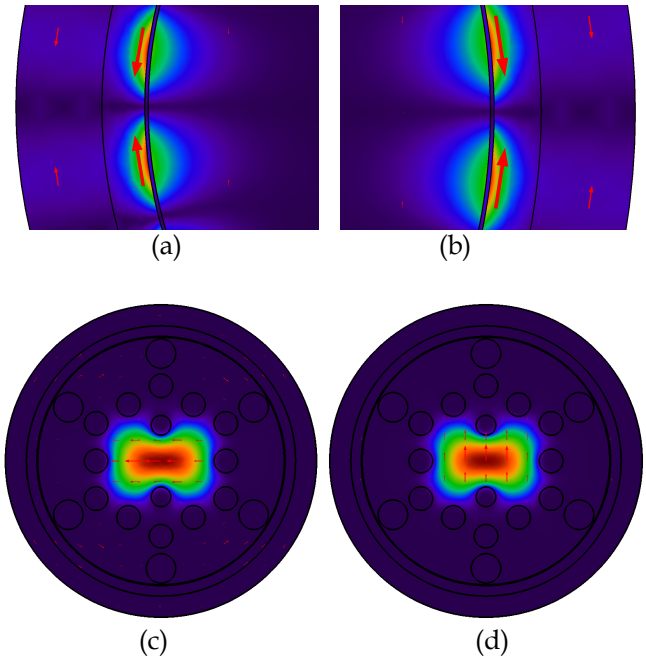

Figure 2. Electro field distribution on the sensor surface (a) Left Spp-mode, (b) Right Spp-mode, (c) x-polarization, and (d) y-polarization

During the numerical simulation, the proposed sensor component has a consistent value in detecting changes in concentration in a mixture of alcohol and water at low temperatures. The proposed sensor component can detect analytes in the range of refractive index 1.30 – 1.39 RIU, and found a maximum sensitivity of 12,000 nm/RIU (Irawan, Ramadhan, Saktioto, Fitmawati, et al., 2022b). In this case, we perform simulations for each concentration of a mixture of alcohol and water at a temperature of 20 ^{0}C. We converted the concentration of a mixture of alcohol and water to the refractive index which also has been reported in previous studies. The conversion can be seen in table 1. The concentration range tested in this study were 15%, 40%, 60%, and 70%. As in table 1, the refractive index for each analyte concentration has a very small difference and is in the range of refractive index 1.34361 to 1.36472 (Qiu et al., 2020).

In Figure 3 we find the relationship between the wavelength of the proposed sensor and the concentration of a mixture of alcohol and water on x-polarization. At a concentration of 15% the proposed sensor component has a peak confinement loss of 392.3 dB/cm, and it is known that the resonance wavelength is at 620 nm, meanwhile, when the analyte concentration is increased to 40%, the sensor component provides information that the confinement loss peak is 587.64 dB/cm, and the resonance wavelength shifted by 400 nm to 660 nm. In this concentration change, it is known that the refractive index has a change of 0.01494 RIU. then the alcohol concentration was increased to 60% in order to

obtain a resonance wavelength at 670 nm and a confinement loss peak of 733.65 dB/cm. In this range, the resonance wavelength only shifts by 100 nm, and it is known that the refractive index change is 0.00481 RIU. finally, we tested to increase the concentration of the mixture of alcohol and water by 70%. In this range, we find that there is no shift in the resonance wavelength and only a change in confinement loss of 723.75 dB/cm. Confinement loss has decreased in this phase.

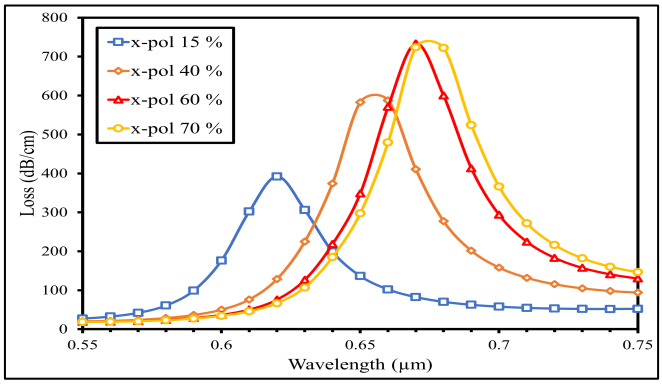

Figure 3. Loss on x-pol vs concentration ethyl alcohol-water mixtures

Furthermore, we have observed changes in the concentration of a mixture of alcohol and water on y-polarization. As shown in Figure 4. Y-polarization on the proposed PCF-SPR sensor component shows the same tendency to detect any change in analyte concentration. What is significantly different from x-polarization is the confinement loss value. In y-polarization confinement loss on the sensor, the component has a higher value than the confinement loss in x-polarization, meanwhile, the resonance wavelength of each concentration has the same value, namely at 15%, 40%, 60%, and 60% analyte concentrations, respectively. 70% found resonance wavelengths at 620 nm, 660 nm, 670 nm, and 670 nm. Using equation 4, we find that the proposed sensor component has a sensitivity in detecting analyte concentration of 91 nm/% (Wang et al., 2021).

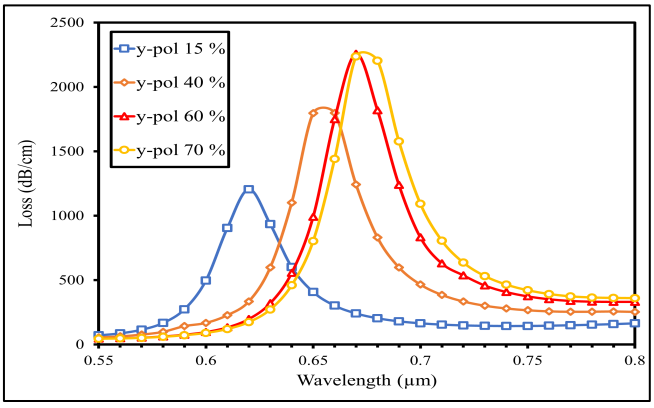

Figure 4. Loss of y-pol vs concentration of ethyl alcohol-water mixtures

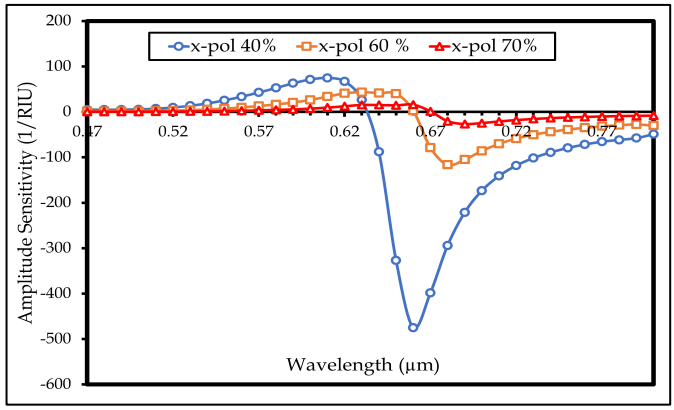

Figure 5. Relationship of amplitude sensitivity vs concentration ethyl alcohol-water mixtures

Next, we make observations on the amplitude sensitivity of the proposed sensor in detecting the analyte concentration. In Figure 5 we show the relationship between the amplitude sensitivity x-polarization sensor proposed for detecting the analyte concentration. Amplitude sensitivity is one of the effective Sensing in analyzing analyte changes, amplitude sensitivity is obtained from equation 5. At 40% analyte concentration, the amplitude sensitivity peak is -474,875 1/RIU and is at a wavelength of 660 nm, meanwhile, when the analyte concentration is increased to 60%, the peak amplitude sensitivity was obtained at -116.3 1/RIU, meanwhile, the wavelength shifted by 200 nm and was obtained at 680 nm. Finally, when the concentration was increased to 70%, the amplitude was obtained at -26.76 1/RIU, while the wavelength was at 690 nm (Jabin et al., 2019).

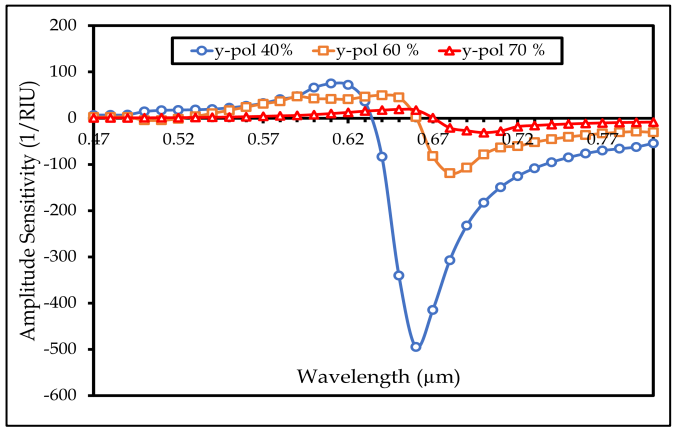

Figure 6. Relationship of amplitude sensitivity vs ethyl alcohol-water mixtures

Finally, we observed the y-polarization in Figure 6, in general, the amplitude sensitivity value and wavelength shift are the same as the x-polarization, the greater the concentration the smaller the confinement loss peak, however, there are differences in the amplitude sensitivity and wavelength values at a concentration of 70%. Y-pol amplitude sensitivity at

40%, 60%, and 70% analyte concentrations were -495 1/RIU, -119 1/RIU, and -31.3 1/RIU, respectively. The difference occurred when the analyte concentration at 70% wavelength was found at the y-polarization of 700 nm.

Conclusions

In detecting alcohol concentration, we have proposed a PCF-SPR sensor with a simple geometric structure to be used as a sensing component. In this work, we have investigated the performance of a dual-polarized PCF-SPR sensor in detecting alcohol concentration in numerical simulation using the finite element method. We found that the proposed sensor can detect changes in concentration in a mixture of water and alcohol with a sensitivity of 91 nm/%. We observed in two techniques, namely the wavelength technique (WS) and the amplitude sensitivity technique (AS).

Acknowledgments

We would like to thank LPPM Universitas Riau for their great support and We also would like to thank Optics and Optoelectronics laboratory and the plasma and photonics physics laboratory.

References

Hsu, C. Y., Chiang, C. C., Hsieh, T. S., Hsu, H. C., Tsai, L., & Hou, C. H. (2021). Study of fiber Bragg gratings with TiN-coated for cryogenic temperature measurement. *Optics and Laser Technology*, *136*. https://doi.org/10.1016/j.optlastec.2020.106768

Irawan, D., Azhar, A., & Ramadhan, K. (2022). High-Performance Compensation Dispersion with Apodization Chirped Fiber Bragg Grating for Fiber Communication System. *Jurnal Penelitian Pendidikan IPA*, *8*(2), 992–999. https://doi.org/10.29303/jppipa.v8i2.1521

Irawan, D., Ramadhan, K., & Azhar, A. (2022). Optimum Design Sapphire-Fiber Bragg Grating for High-Temperature Sensing. *Jurnal Penelitian Pendidikan IPA*, *8*(3), 1361–1367. https://doi.org/10.29303/jppipa.v8i3.1663

Irawan, D., Ramadhan, K., Saktioto, S., Fitmawati, F., Hanto, D., & Widiyatmoko, B. (2022a). Hexagonal two layers-photonics crystal fiber based on surface plasmon resonance with gold coating biosensor easy to fabricate. *Indonesian Journal of Electrical Engineering and Computer Science*, *28*(1), 146. https://doi.org/10.11591/ijeecs.v28.i1.pp146-154

Irawan, D., Ramadhan, K., Saktioto, S., & Marwin, A. (2022). Performance comparison of Topas chirped fiber bragg grating sensor with tanh and gaussian apodization. *Indonesian Journal of Electrical Engineering and Computer Science*, *26*(3), 1477–1485. https://doi.org/10.11591/ijeecs.v26.i3.pp1477-1485

Irawan, D., Ramadhan, K., Saktioto, T., Fitmawati, F., Hanto, D., & Widiyatmoko, B. (2022b). High-Performance of Star-Photonics Crystal Fiber Based on Surface Plasmon Resonance Sensor. *Indian Journal of Pure & Applied Physics*, *60*(9), 727–733. https://doi.org/https://doi.org/10.56042/ijpap.v60i9.64411

Islam, M. R., Iftekher, A. N. M., Hasan, K. R., Nayen, M. J., Islam, S. Bin, Hossain, A., Mustafa, Z., & Tahsin, T. (2021). Design and numerical analysis of a gold-coated photonic crystal fiber based refractive index sensor. *Optical and Quantum Electronics*, *53*(2). https://doi.org/10.1007/s11082-021-02748-8

Jabin, M. A., Ahmed, K., Rana, M. J., Paul, B. K., Islam, M., Vigneswaran, D., & Uddin, M. S. (2019). Surface Plasmon Resonance Based Titanium Coated Biosensor for Cancer Cell Detection. *IEEE Photonics Journal*, *11*(4). https://doi.org/10.1109/JPHOT.2019.2924825

Korganbayev, S., Orazayev, Y., Sovetov, S., Bazyl, A., Schena, E., Massaroni, C., Gassino, R., Vallan, A., Perrone, G., Saccomandi, P., Arturo Caponero, M., Palumbo, G., Campopiano, S., Iadicicco, A., & Tosi, D. (2018). Detection of thermal gradients through fiber-optic Chirped Fiber Bragg Grating (CFBG): Medical thermal ablation scenario. *Optical Fiber Technology*, *41*, 48–55. https://doi.org/10.1016/j.yofte.2017.12.017

Lu, Y., Wang, M. T., Hao, C. J., Zhao, Z. Q., & Yao, J. Q. (2014). Temperature Sensing Using Photonic Crystal Fiber Filled With Silver Nanowires and Liquid. *IEEE Photonics Journal*, *6*(3). https://doi.org/10.1109/JPHOT.2014.2319086

Mohapatra, A. G., Talukdar, J., Mishra, T. C., Anand, S., Jaiswal, A., Khanna, A., & Gupta, D. (2022). Fiber Bragg grating sensors driven structural health monitoring by using multimedia-enabled iot and big data technology. *Multimedia Tools and Applications*. https://doi.org/10.1007/s11042-021-11565-w

Mou, F. A., Rahman, M. M., Islam, M. R., & Bhuiyan, M. I. H. (2020). Development of a photonic crystal fiber for THz wave guidance and environmental pollutants detection. *Sensing and Bio-Sensing Research*, *29*. https://doi.org/10.1016/j.sbsr.2020.100346

Qiu, S., Yuan, J., Zhou, X., Qu, Y., Yan, B., Wu, Q., Wang, K., Sang, X., Long, K., & Yu, C. (2020). Highly sensitive temperature sensing based on all-solid cladding dual-core photonic crystal fiber filled with the toluene and ethanol. *Optics Communications*, *477*.

https://doi.org/10.1016/j.optcom.2020.126357

Rahman, M. T., Datto, S., & Sakib, M. N. (2021). Highly sensitive circular slotted gold-coated micro channel photonic crystal fiber based plasmonic biosensor. *OSA Continuum*, *4*(6), 1808. https://doi.org/10.1364/osac.425279

Ramadhan, K. (2020). Dispersi multi-layer pada inti serat optik moda tunggal. *Seminar Nasional Fisika Universitas Riau V (SNFUR-5)*, 1–5.

Ramadhan, K., & Saktioto, T. (2021). Integrasi Chirping dan Apodisasi Bahan TOPAS untuk Peningkatan Kinerja Sensor Serat Kisi Bragg. *Komunikasi Fisika Indonesia*, *18*(2), 111–123. https://doi.org/http://dx.doi.org/10.31258/jkfi.18.2.111-123

Rifat, A. A., Mahdiraji, G. A., Ahmed, R., Chow, D. M., Sua, Y. M., Shee, Y. G., & Adikan, F. R. M. (2016). Copper-graphene-based photonic crystal fiber plasmonic biosensor. *IEEE Photonics Journal*, *8*(1). https://doi.org/10.1109/JPHOT.2015.2510632

Saktioto, T., Ramadhan, K., Soerbakti, Y., Irawan, D., & Okfalisa. (2021a). Apodization sensor performance for TOPAS fiber Bragg grating. *Telkomnika*, *19*(6). https://doi.org/http://dx.doi.org/10.12928/telkomnika.v19i6.21669

Saktioto, T., Ramadhan, K., Soerbakti, Y., Irawan, D., & Okfalisa. (2021b). Integration of chirping and apodization of Topas materials for improving the performance of fiber Bragg grating sensors. *Journal of Physics: Conference Series*, *2049*(1). https://doi.org/10.1088/1742-6596/2049/1/012001

Sen, S., Abdullah-Al-Shafi, M., Sikder, A. S., Hossain, M. S., & Azad, M. M. (2021). Zeonex based decagonal photonic crystal fiber (D-PCF) in the terahertz (THz) band for chemical sensing applications. *Sensing and Bio-Sensing Research*, *31*. https://doi.org/10.1016/j.sbsr.2020.100393

Shakya, A. K., Ramola, A., Singh, S., & Van, V. (2022). Design of an ultra-sensitive bimetallic anisotropic PCF SPR biosensor for liquid analytes sensing. *Optics Express*, *30*(6), 9233. https://doi.org/10.1364/oe.432263

Wang, J. K., Ying, Y., Hu, N., & Cheng, S. Y. (2021). Double D-shaped optical fiber temperature and humidity sensor based on ethanol and polyvinyl alcohol. *Optik*, *242*. https://doi.org/10.1016/j.ijleo.2021.166972

Wu, T., Shao, Y., Wang, Y., Cao, S., Cao, W., Zhang, F., Liao, C., He, J., Huang, Y., Hou, M., & Wang, Y. (2017). Surface plasmon resonance biosensor based on gold-coated side-polished hexagonal structure photonic crystal fiber. *Optics Express*, *25*(17), 20313. https://doi.org/10.1364/oe.25.020313